10.1098/rspa.2001.0832

Vertical jets from standing waves. II

By Michael S. Longuet-Higgins[1] and Douglas G. Dommermuth[2]

[1] *Institute for Nonlinear Science, University of California, San Diego, La Jolla, CA 92093-0402, USA*

[2] *Naval Hydrodynamics Division, Science Applications International Corporation, 10260 Campus Point Drive, San Diego, CA 92121, USA*

Received 6 March 2001; accepted 3 April 2001

In a previous paper it was shown that in steep standing waves on water the collapse of a rounded cavity in the wave trough can produce quite high local vertical accelerations, initiating the growth of a strong vertical jet. In one example given here, the acceleration exceeds $100g$. The main purpose of the present paper is to follow the subsequent development of the jet by means of a boundary-integral time-stepping technique. It is found that the jets tend to bifurcate into two halves, each forming a plunging or spilling breaker. The transition of the rising wave trough into a thin jet is here compared with an asymptotic flow in which the free surface is given by a quartic equation.

Keywords: water waves; surface waves; jet formation; wave breaking; standing waves; vertical acceleration

1. Introduction

In a recent paper (Longuet-Higgins 2001*a*, hereafter referred to as paper I) it was shown that steep standing waves on the surface of deep water can, in some circumstances, produce remarkably large vertical accelerations, giving rise to vertical jets of water arising out of the wave troughs. A similar phenomenon could occur through the impact of a water wave against a vertical wall or cliff face or against the side of a ship in deep water. A sufficient condition for moderately large accelerations is that the wave trough have the form of an almost circular arc, as in a shaped charge.

The previous calculations were carried out using a new method due essentially to Balk (1996), which is particularly convenient for parametrizing the initial conditions for the flow. The examples given in paper I showed that the resulting vertical accelerations of a particle in the wave trough could exceed $10g$, before falling off rapidly to smaller values.

After the acceleration had fallen to near zero, the tip of the jet began to develop a sharp curvature. For the mathematical description of such a sharp corner, Balk's analysis, which is in terms of a Fourier series, is not so well adapted. In fact the calculations tended to lose accuracy slightly before the sharp corner was formed.

The purpose of the present paper is to continue and extend the previous results by making use of another but complementary method of numerical time-stepping, which was devised for the study of breaking waves by Longuet-Higgins & Cokelet (1976). This boundary-integral technique has been further developed by many authors: see, for example, Vinje & Brevig (1981), Dold & Peregrine (1986), Roberts (1983) and Mercer & Roberts (1992). In the present paper we shall make use of an accurate version of Vinje & Brevig's formulation, which has been used previously to follow the nonlinear development of steep gravity waves when subjected to a normal-mode perturbation (Longuet-Higgins & Dommermuth 1997). It can equally well be used to study the time-history of any space-periodic surface waves, and in particular to follow the standing-wave jets that concern us here.

2. Initial conditions

In paper I the horizontal and vertical coordinates (x, y) of a point on the free surface were given in general by equations of the form

$$\left.\begin{aligned} x &= \xi + \sum_{n=1}^{N} n^{-1} a_n \sin n\xi, \\ y &= y_0 + \sum_{n=1}^{N} n^{-1} a_n \cos n\xi, \end{aligned}\right\} \tag{2.1}$$

where ξ is a parameter running from 0 to 2π over one wavelength $L = 2\pi$, and the coefficients $a_n(t)$ are functions of the time t only. Moreover, to conserve the total mass of fluid,

$$y_0 = -\sum_{n=1}^{N} \frac{1}{2n} a_n^2. \tag{2.2}$$

In the present system, the initial conditions are specified by the values of the coordinates (x, y) of each point on the surface at time $t = 0$, together with the velocity potential at the free surface. In all of the examples considered here, the initial velocity is zero. Hence we may simply take

$$\dot{a}_n(0) = 0, \quad n = 1, 2, \ldots, N. \tag{2.3}$$

The particular examples chosen in paper I had very simple initial conditions. In the first four examples A, B, C and D we took $N = 2$. The initial values of the coefficients a_1 and a_2 were given in table 1 of paper I, and will be restated in the figure captions below. They correspond to cases where the total width $2x_1$ of the wave trough is given by

$$x_1/\pi = 0.25,\ 0.20,\ 0.15 \text{ and } 0.10, \tag{2.4}$$

respectively. The time t is measured in units in which the wavenumber k and the acceleration due to gravity g are both equal to 1.

3. Results

Figure 1 shows the development of the surface profile in case A , $x_1/\pi = 0.25$, from $t = 0$–2.4 at intervals of 0.2. A little more than half a wavelength is shown. When $t = 0$, the wave trough between $x/L = 0.375$ and 0.625 is very nearly circular. The 'crest' arising out of the wave trough first develops a sharp corner at around $t = 1.0$ (the limit of the previous calculations). At around $t = 1.2$ a small protrusion arises

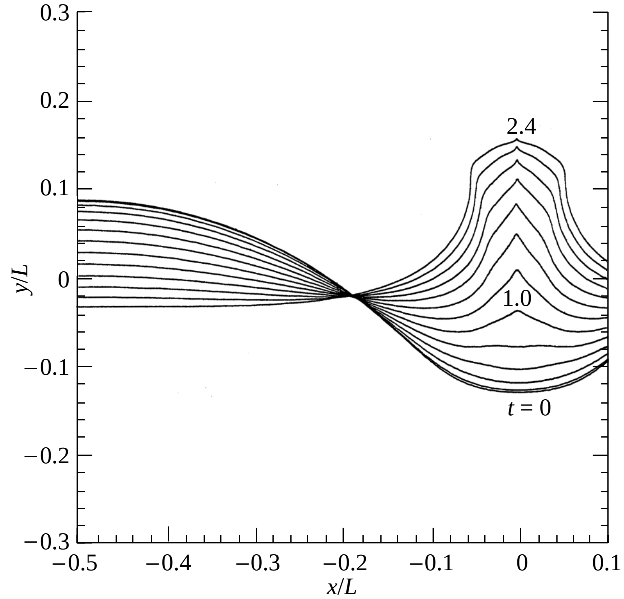

Figure 1. Profiles of the free surface at times $t = 0$ (0.2) 2.4 in case A, $x_1/L = 0.25$. Initial values: $a_1 = 0.6879$, $a_2 = 0.2379$ and $\dot{a}_1 = \dot{a}_2 = 0$.

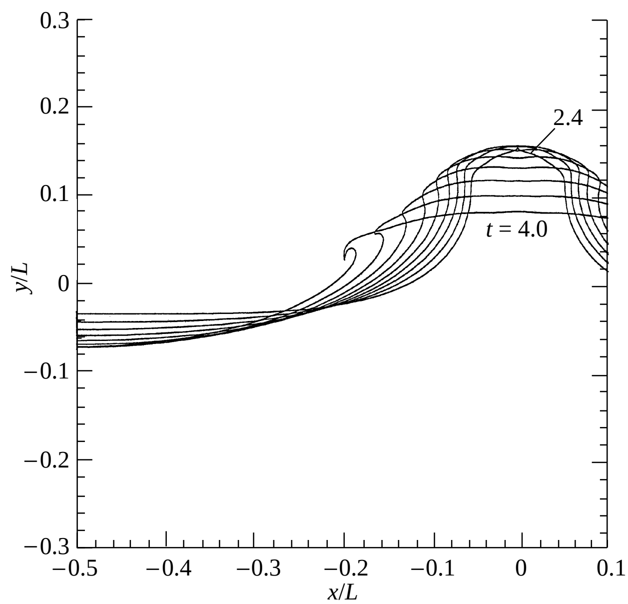

Figure 2. Continuation of figure 1, (case A) $t = 2.4$ (0.2) 4.0.

out of the crest and then becomes sharper ($t = 1.4$ and 1.6), while the main body of the crest thickens and continues to rise. By the time $t = 2.4$ it appears that the sharp tip of the jet is being reabsorbed by the main body.

In figure 2 it can be seen that after $t = 2.4$ the tip is completely reabsorbed, while on each side the surface overturns as in a plunging breaker. The calculation could

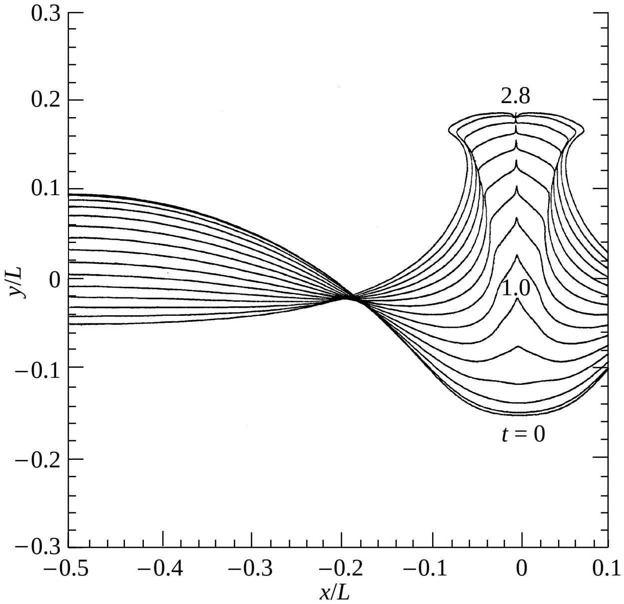

Figure 3. Profiles of the free surface at times $t = 0$ (0.2) 2.8 in case B, $x_1/L = 0.20$. Initial values $a_1 = 0.7815$, $a_2 = 0.2764$ and $\dot{a}_1 = \dot{a}_2 = 0$.

not be continued much beyond $t = 4.0$, owing to the sharp curvature at the tips of the two breakers.

The corresponding acceleration $\ddot{y}$ of the particle at the central point ($y/L = 0.5$) is shown in figure 12, curve A. The acceleration $\ddot{y}$ reaches a peak of about $2.8g$ at around $t = 0.75$, when the free surface is still nearly flat locally, and then falls abruptly to $-g$, when the sharp-pointed tip is formed. In other words, that part of the fluid is in free-fall. The acceleration remains at $-g$ until $t = 2.5$, when the sharp tip has been reabsorbed into the main jet. The acceleration remains negative, however, until after $t = 4.0$.

Next consider case B, when $x_1/L = 2.0$; the initial width of the trough is only one-fifth of the wavelength. Figure 3 shows the jet developing more rapidly than in case A, but otherwise in a similar way. The sharp tip that is formed between $t = 0.8$ and 1.0 rises higher, and when it falls back into the main body it produces a small circular cavity, shown enlarged in figure 4. This reabsorption of the mini-jet can be viewed as the same process as the 'shaped charge' effect, but in reverse.

The vertical acceleration for case B is shown in figure 12, curve B. This time $\ddot{y}$ rises to almost $5g$ at around $t = 0.71$, before falling to $-g$ and remaining there till after $t = 2.8$; throughout this time the tip of the jet is in free-fall.

The very small scale of the features near the cavity in figure 4 prevents the computation in this case being carried beyond about $t = 3.1$. However, on the reasonable assumption that this small part of the flow does not significantly affect the development of the rest of the profile we may cut out a small central section of total width 0.01, say, and splice both y and ϕ across the gap, using a simple interpolation formula, before continuing the time-stepping. This procedure yields figure 5. An enlarged view (figure 6) shows the detail of one of the overturning jets for two different grid solutions.

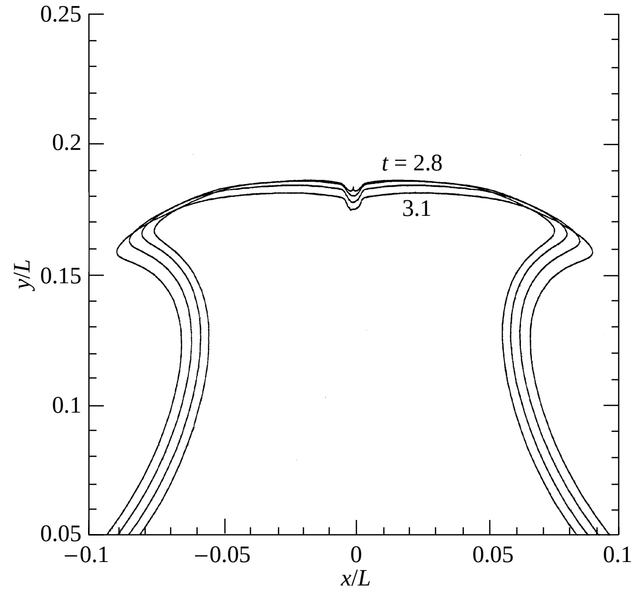

Figure 4. Enlargement of the top of the jet in figure 3 at time $t = 2.8$ (0.1) 3.1.

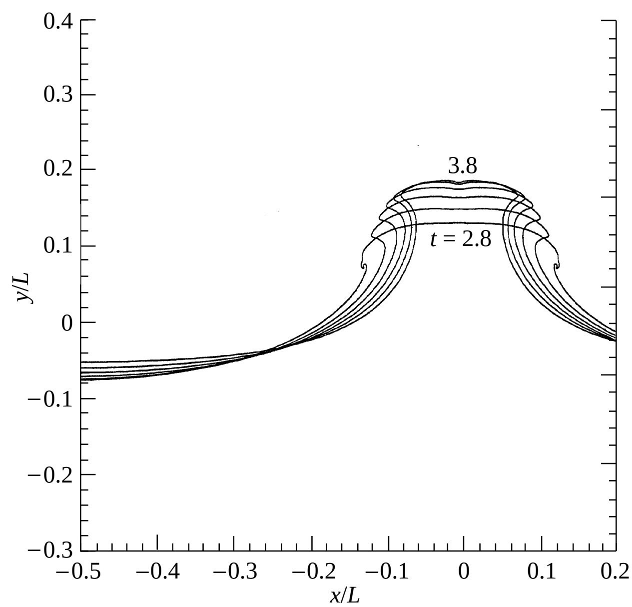

Figure 5. Continuation of figure 3 after cutting and splicing a narrow central section ($|x| \leqslant 0.1$).

In case C, when $x_1/L = 0.15$, the corresponding profiles are shown in figures 7–10. From figure 7 we see that the tip of the jet is reabsorbed at around $t = 2.0$. The maximum vertical acceleration, from figure 12, curve C, is now greater than $8g$.

Again, to carry the computation beyond $t = 2$ it was necessary to cut and splice a narrow section of the profile including the small cavity, as in figure 8. The resulting

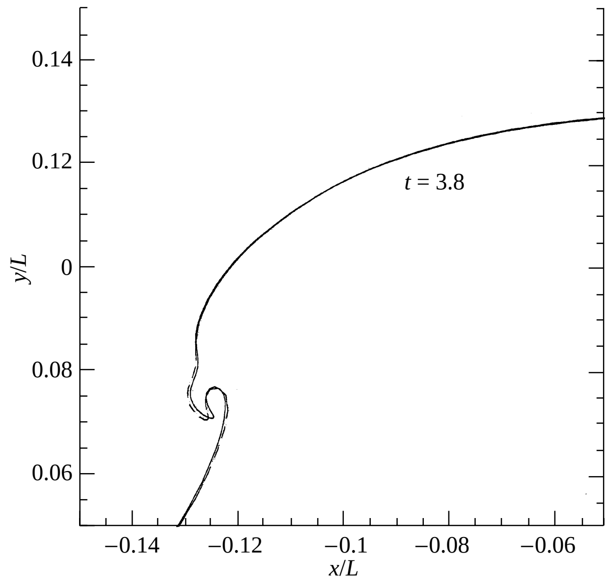

Figure 6. Enlargement of the overturning jet in figure 5 (case C) at $t = 3.8$ (– – –, 256 points; ——, 512 points).

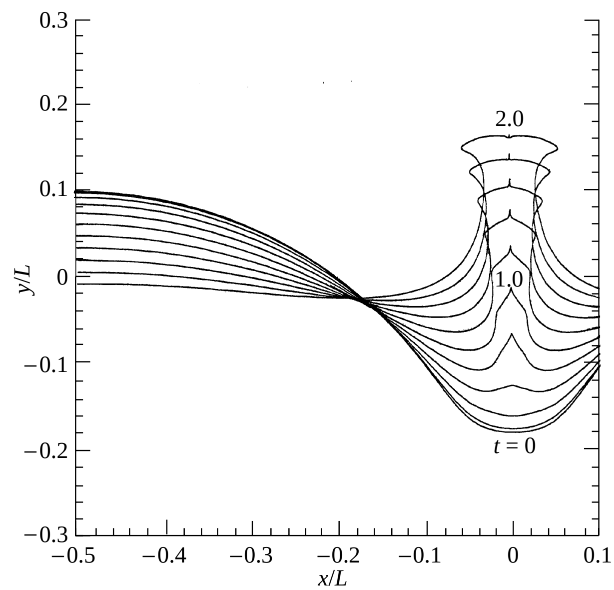

Figure 7. Profiles of the free surface at times $t = 0$ (0.2) 2.0 in case C, $x_1/L = 0.15$. Initial values: $a_1 = 0.8779$, $a_2 = 0.3112$ and $\dot{a}_1 = \dot{a}_2 = 0$.

profiles are shown in figures 9 (centre rising) and figure 10 (centre falling). The side jets clearly become very sharp pointed and thin.

Case D, when $x_1/L = 0.10$, shows a somewhat different behaviour. Figure 11 suggests that the sharp tip does not have time to develop before it is overtaken by the main body of the jet. The absence of this feature enables us to continue the

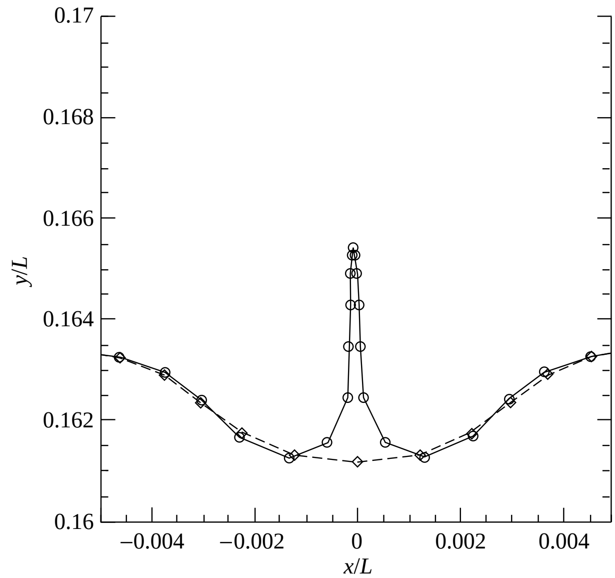

Figure 8. Splicing the central section of figure 7 at $t = 2.0$ (——, original; – – –, splice).

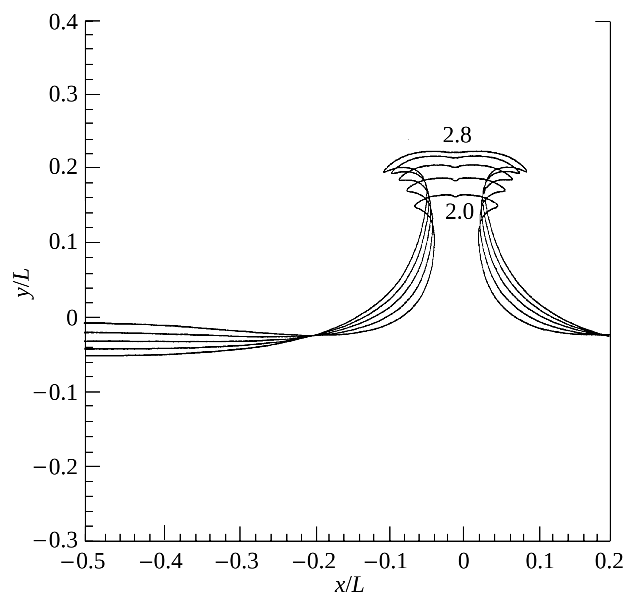

Figure 9. Continuation of figure 7 (case C) after splicing.

calculation until the plunging breakers on each side develop very sharp corners. This time the vertical acceleration $\ddot{y}$ rises to over $10g$.

Figure 12 combines and compares the acceleration curves for all the cases A–D considered so far. It is essentially an extension of fig. 8 in paper I to negative values of $\ddot{y}$ (and larger values of t) and confirms very satisfactorily the agreement between the two quite different methods of numerical calculation.

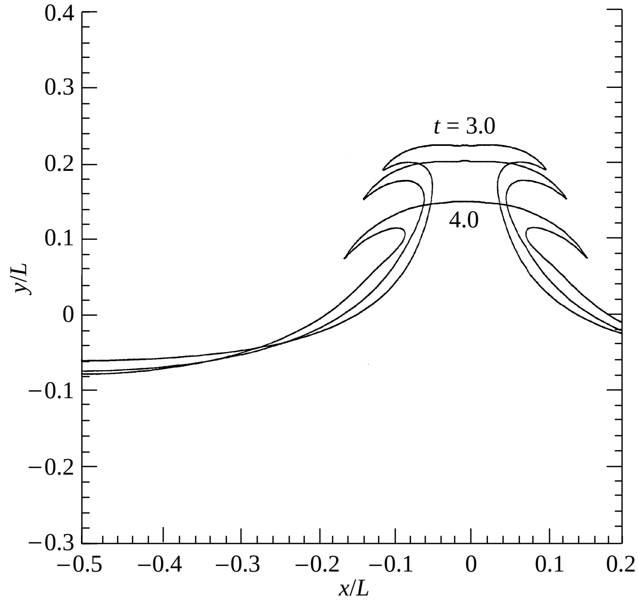

Figure 10. Continuation of figure 9 (case C).

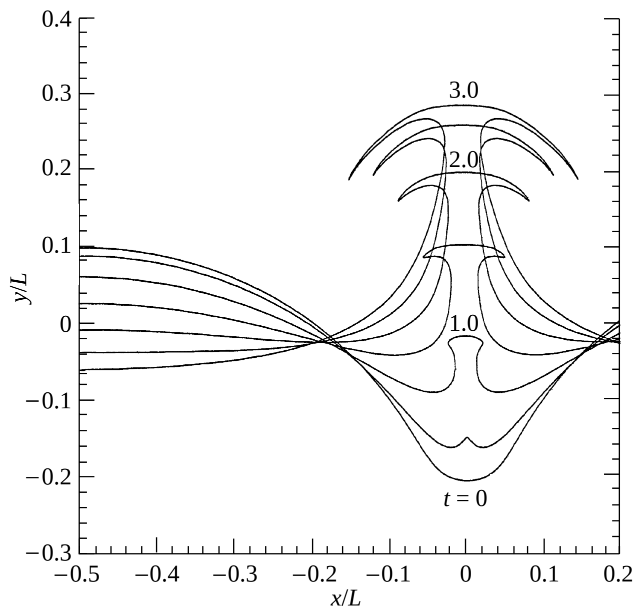

Figure 11. Profiles of the free surface at times $t = 0$ (0.5) 3.0 in case D, $x_1/L = 0.10$. Initial values: $a_1 = 0.9701$, $a_2 = 0.3270$ and $\dot{a}_1 = \dot{a}_2 = 0$.

4. Transition to a jet

One of the most interesting features of the profiles in figures 1, 3, 7 and 11 is the smooth transition of the rising trough from a sharp corner, with slope angle less than 45°, to a more narrow, sharp-tipped jet. In figure 7, for example, this occurs between

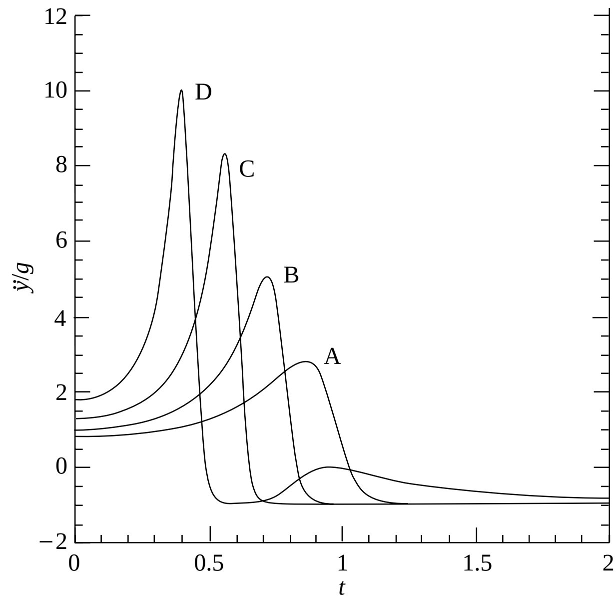

Figure 12. The vertical acceleration as a function of the time in cases A–D.

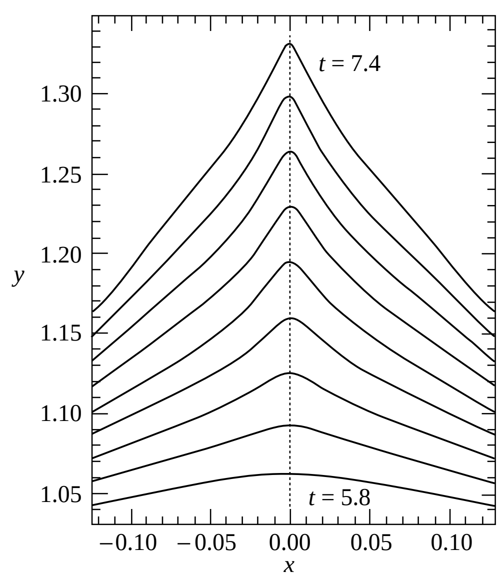

Figure 13. Intermediate profiles in case C at intervals of $\Delta t = 0.02$, showing the transition from a sharp corner to a jet.

$t = 0.6$ and 0.8. An enlargement, with intermediate profiles at intervals $\Delta t = 0.05$, is shown in figure 13. It is notable that there is no discontinuity at the instant when the angle of maximum slope is 45°, as there is in a Dirichlet hyperbola (Longuet-Higgins 1972). Instead, the sequence of profiles more closely resembles one of the canonical forms for the development of a sharp-pointed jet which have been derived in a recent

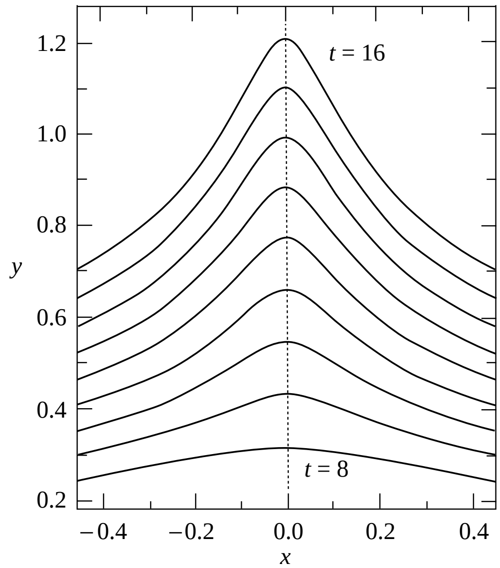

Figure 14. Profiles given by the asymptotic expression (4.1) when $\gamma = -6$, at intervals of $\Delta t = 1.0$.

paper (Longuet-Higgins 2001*b*). These are given by the quartic equation

$$x^2 = \pm\delta t^{-2} - (y^3 + 9x^2 y)/t + [(7\gamma - \tfrac{9}{2})x^4 - 9(2\gamma + 1)x^2 y^2 - (\gamma + \tfrac{9}{2})y^4]/t^2, \quad (4.1)$$

where x and y are horizontal and vertical coordinates in a free-fall frame of reference, and $\delta = \pm 1$ and γ is an arbitrary dimensionless constant. Expression (4.1) is valid asymptotically for small values of x/t and y/t. The scales of length and time, and the value of γ, are chosen so as to match the outer flow. An example is shown in figure 14, where $\gamma = -6.0$. A uniform vertical velocity $V = 0.05$ has been imposed. To make figures 13 and 14 directly comparable, the profiles in figure 13 have been replotted in an inertial frame of reference, by giving each curve a uniform vertical displacement $\frac{1}{2}g(t - t_1)^2$, where $g = 1$ and $t_1 = 0.6$.

Similar comparisons can be made between equation (4.1) and the profiles in figures 1, 3 and 11 at the appropriate times.

5. Example of an extremely high acceleration

So far we have assumed the maximum number N of harmonics in our representation (2.1) of the initial conditions to be just 2. Consider, however, a case when $N = 3$, namely let

$$a_1 = \tfrac{5}{8}, \qquad a_2 = -\tfrac{2}{8}, \qquad a_3 = -\tfrac{3}{8}, \quad (5.1)$$

with $\dot{a}_n(0) = 0$, $n = 1, 2, 3$, as before. Figures 15 and 16 show that the initial wave trough is very flat, with two rather sharp corners at each end. Each corner is roughly the arc of a circle. When $t > 0$, each corner collapses at first independently of the other, but then the two resulting jets converge to form a smaller semicircular trough near the centre. This gives rise to extremely high accelerations, $\ddot{y}$ exceeding $400g$ (see figure 17). The calculations cease at around $t = 0.54 = t_c$, say. A logarithmic

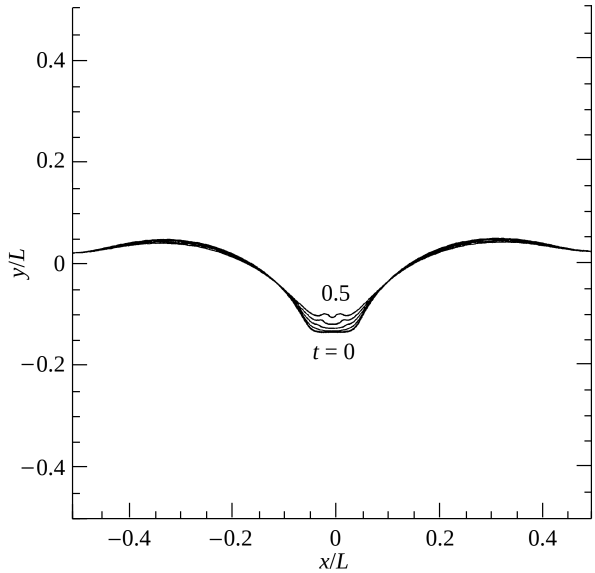

Figure 15. Profiles of the free surface at times $t = 0\ (0.1)\ 0.5$ with initial conditions $a_1 = \frac{5}{8}$, $a_2 = -\frac{2}{8}$, $a_3 = -\frac{3}{8}$ and $\dot{a}_1 = \dot{a}_2 = \dot{a}_3 = 0$.

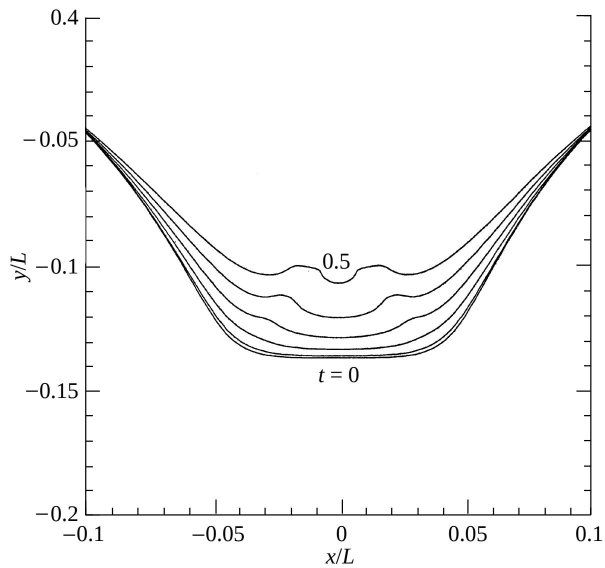

Figure 16. Enlargement of the central portion of figure 15.

plot is interesting. In figure 18 we have plotted $\ln(\ddot{y}/g)$ against $\ln|t_c - t|$. It can be seen that the plot is linear over $1\frac{1}{2}$ decades, showing that

$$\ddot{y}/g \propto |t_c - t|^{\beta} \tag{5.2}$$

over this range of t. This type of power-law behaviour has been shown to be typical of free-surface flows that are close to being critical, in the sense that they almost pinch off a 'bubble of air' (see Longuet-Higgins & Oguz 1997).

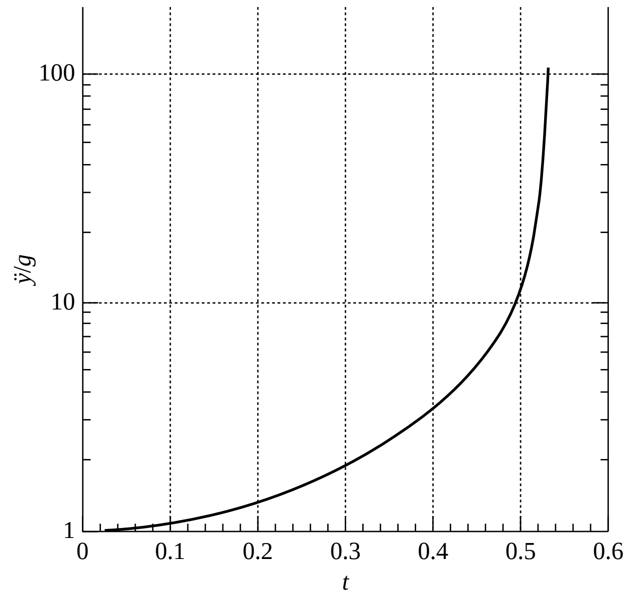

Figure 17. The vertical acceleration of a particle on the central line in figures 15 and 16, as a function of t.

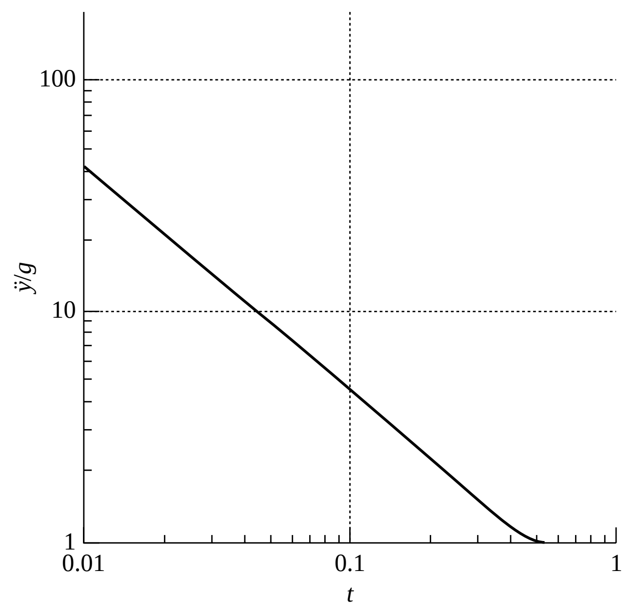

Figure 18. Logarithmic plot of $\ddot{y}/g$ against $|t - t_c|$, where $t_c = 0.54$.

6. Conclusion

When a standing gravity wave is allowed to develop from a rounded cavity, the vertical acceleration may attain quite high values compared with g. However, in the subsequent development of the jet the accelerations are relatively small and the tip of the jet is practically in free-fall. In the examples given here the jet bifurcates into two plunging or spilling breakers falling away to either side. As shown elsewhere (Longuet-Higgins & Dommermuth 2001), other initial conditions can give rise to single, sharp-pointed jets, which relapse into the surface and form a temporary cavity: a time-reversal of the cases discussed here. Both types of behaviour seem to have been observed by Jiang *et al*. (1998) in their experiments on subharmonically forced standing waves. However, a full dynamical explanation of these authors' observations has yet to be given.

The calculations in §§ 3–5 were presented at the IUTAM Symposium on Free-Surface Flows, Birmingham, UK, in July 2000. M.S.L-H. is supported by the Office of Naval Research under contract N00014-00-1-0248. D.G.D. is supported under contract N00014-97-C-0345.

References

Balk, A. M. 1996 A Lagrangian for water waves. *Phys. Fluids* **8**, 416–420.

Dold, J. W. & Peregrine, D. H. 1986 An efficient boundary-integral method for steep, unsteady water waves. In *Numerical methods for fluid dynamics* (ed. K. W. Morton & M. J. Baines), vol. II, pp. 671–679. Oxford University Press.

Jiang, L., Perlin, M. & Schultz, W. W. 1998 Period tripling and energy dissipation of breaking standing waves. *J. Fluid Mech.* **369**, 273–299.

Longuet-Higgins, M. S. 1972 A class of exact, time-dependent free-surface flows. *J. Fluid Mech.* **55**, 529–543.

Longuet-Higgins, M. S. 2001*a* Vertical jets from standing waves. *Proc. R. Soc. Lond.* A **457**, 495–510.

Longuet-Higgins, M. S. 2001*b* Asymptotic forms for jets from standing waves. *J. Fluid Mech.* (In the press.)

Longuet-Higgins, M. S. & Cokelet, E. D. 1976 The deformation of steep surface waves on water. *Proc. R. Soc. Lond.* A **350**, 1–26.

Longuet-Higgins, M. S. & Dommermuth, D. G. 1997 Crest instabilities of gravity waves. Part 3. Nonlinear development and breaking. *J. Fluid Mech.* **336**, 33–50.

Longuet-Higgins, M. S. & Dommermuth, D. G. 2001 On the breaking of standing waves by falling jets. *Phys. Fluids* **13**, 1652–1659.

Longuet-Higgins, M. S. & Oguz, H. N. 1997 Critical jets in surface waves and collapsing cavities. *Phil. Trans. R. Soc. Lond.* A **355**, 625–639.

Mercer, G. N. & Roberts, A. J. 1992 Standing waves in deep water: their stability and extreme form. *Phys. Fluids* A **4**, 259–269.

Roberts, A. J. 1983 A stable and accurate numerical method to calculate the motion of a sharp interface between fluids. *IMA J. Appl. Math.* **31**, 13–35.

Vinje, T. & Brevig, P. 1981 Breaking waves on finite water depths: a numerical study. Report R-111.81, Ship Research Institute of Norway.